Journal of Applied Electrochemistry **29**: 719–727, 1999.

Influence of Zn^{2+} ions on copper electrowinning from sulfate electrolytes

L. MURESAN[1]*, A. NICOARA[1], S. VARVARA[1] and G. MAURIN[2]
[1]*Faculty of Chemistry and Chemical Engineering, Babes-Bolyai University, str. Arany Janos nr. 11, 3400 Cluj-Napoca, Romania;*
[2]*UPR 15 du CNRS: 'Physique des Liquides et Electrochimie', Tour 22, 4 Place Jussieu, 75252 Paris, France*
*(*author for correspondence, e-mail: limur@chem.ubbcluj.ro)*

Received 1 April 1998; accepted in revised form 1 September 1998

Key words: copper electrowinning, impedance spectroscopy, sulphate electrolyte, Zn^{2+} ions

Abstract

During electrowinning of copper from wastes, it was observed that Zn^{2+} impurities had some effects on the aspect of the deposits although the codeposition of these two metals is impossible under normal conditions. Cyclic voltammetry, impedance analysis and rotating disc electrode techniques were used to characterize the effect of the presence of small amounts of Zn^{2+} on the copper electrodeposition kinetics from acidic sulphate electrolytes. SEM and X-ray diffraction analysis were used to determine the morphology and the structure of the copper deposits. Their composition was determined using X-ray dispersive analysis. The addition of small amounts of Zn^{2+} had no effect, either on the crystal growth orientation of the copper deposits, or on their composition, but it modified slightly their morphology by increasing their microscopic roughness. An increase in the cathodic peak of the cyclic voltammograms observed in the presence of Zn^{2+} can be attributed to the higher roughness of the copper deposits. From impedance analysis, it can be deduced that Zn^{2+} ions are electrosorbed at the interface and have an effect on the copper electrodeposition kinetics. The adsorption capacitance, C_a, was calculated and correlated with the Zn^{2+} concentration. It was found that the nucleation time constant, parameter influenced by the growing mode of the deposit, decreased in the presence of Zn^{2+}, especially at low concentrations.

1. Introduction

One of the distinguishing features of copper electrowinning, as compared with other electrorefining processes, is the large concentration of impurities present in the electrolyte. During the leaching of the raw materials, many impurities such as Fe^{2+}, Mn^{2+}, Al^{3+}, Ca^{2+}, Ni^{2+}, Co^{2+}, may be dissolved in the electrolyte. Their effects on copper electrowinning have been investigated in terms of current efficiency, deposit morphology and crystal orientation [1]. The subject has been widely studied, because of the decrease in the quantity and quality of the naturally occurring nonferrous resources and also in order to recover metals from waste, both for economic and ecological reasons [2].

Many of the electrochemical difficulties encountered during deposition may be correlated with the concentrations of various species that originate in the ore. Thus, to run the electrowinning process at its maximum efficiency, it is necessary to monitor carefully the behavior of the foreign species.

The Fe^{2+} ion, which is one of the most harmful elements affecting copper electrodeposition, is the most studied impurity [3–6]. Other species, such as As [7, 8], Sb [8], Bi [8] and Ni [9], are also known to have a deleterious effect on the structure of the copper electrodeposit. The influence of some electroinactive cations, such as NH_4^+, Na^+, K^+ and Li^+ has also been studied. It has been shown that they modify the nucleation mechanism, the nucleation rate and the growth mechanism and, therefore, the deposit morphology [10].

The present study deals with the specific effects of Zn^{2+} ions during copper electrodeposition. Zinc is present in large amounts in industrial wastes resulting from the thermometallurgical processing of nonferrous ores at Copsa-Mica (Romania). The recovery of copper from these wastes is of major interest. An influence of

zinc on copper deposit morphology was detected, although codeposition of this metal with copper is not possible, due to the very different reduction potentials of Zn^{2+} and Cu^{2+} ions.

Cyclic voltammetry, impedance spectroscopy and rotating disc electrode (RDE) techniques were used to characterize the effect of Zn^{2+} on cathodic polarization and copper deposition kinetics. X-ray diffraction, Scanning Electron microscopy (SEM) and X-ray dispersive analysis (EDX) were used to investigate the structure, the morphology and the composition of copper deposits.

2. Experimental details

2.1. *Electrolyte*

A stock solution of acidic copper sulphate was prepared using pure reagents (Merck) and distilled water. The solution contained 30 g dm^{-3} Cu^{2+} as $CuSO_4$ and 100 g dm^{-3} H_2SO_4. Various amounts of a concentrated solution of $ZnSO_4$ were added to obtain electrolytes containing 10 to 500 mg dm^{-3} of Zn^{2+}.

2.2. *Electrochemical cells*

Two kinds of electrochemical cell were used. The first, a parallel plate cell, was equipped with one vertical planar brass sheet cathode between two parallel lead plate anodes. This geometry was adopted to simulate, at a small scale, an industrial cell. Copper was deposited on both sides of the cathode onto a total area of 2.25 cm^2. The cell volume was 0.1 dm^3. The electrolyte was continuously recirculated from a one litre tank.

The second cell was a cylindrical glass vessel ($V = 100$ cm^3) with separated compartments. It was used to perform electrochemical investigations. Copper was electrodeposited onto a Cu disc electrode (2 mm dia.) which was carefully mechanically polished and rinsed before each experiment. The working electrode potential was monitored against a saturated calomel reference electrode (SCE) by means of a potentiostat (PS 3, Meinsberg, Germany). The counter electrode was a platinum grid located in the second compartment of the cell.

2.3. *Examination of deposits*

Morphological examination of the copper deposits prepared in the parallel plate cell were carried out with a Cambridge S 250 scanning electronic microscope. The chemical composition of the samples was obtained using a Tracor–Voyager energy dispersive X-ray analyser coupled with the SEM. The preferential growth axis of the copper deposits was determined by comparing the relative peak intensities of X-ray powder diffraction diagrams according to a method derived in a previous study on lead electrodeposition [11].

2.4. *Cyclic and linear voltammetry*

Cyclic and linear voltammograms were recorded in the second cell, at a scan rate of 20 mV s^{-1} by monitoring the potential with a computer controlled system. The potential range was between 0.75 and −0.75 V vs SCE for the cyclic voltammmetry and between 0 and −0.7 V vs SCE for the linear voltammetry. Experiments were performed on the copper disc cathode which was either motionless or was rotated between 300 and 1300 rpm.

2.5. *Spectroscopy of electrochemical impedance*

Impedance diagrams were recorded in the Nyquist coordinate system in the 3.2 mHz and 10 kHz frequency range by using a 'virtual instrument' frequency response analyzer, developed in our laboratory, based on a AT-MIO 16F5 National Instruments data acquisition board and an Olivetti 440 PC, connected to an analogic potentiostat. For control of the mass transport, the electrode was rotated at 1000 rpm. Measurements were performed under potentiostatic conditions at three different potentials (−0.05, −0.075 and −0.1 V vs SCE) corresponding to moderate cathodic overpotentials. To improve the accuracy, measurements were automatically repeated up to 20 times, especially for high frequency measurements, leading to experiments lasting more than 2 h.

3. Results and discussion

3.1. *Structure of copper deposits*

Copper electrodeposition was carried out in the parallel plate cell using electrolytes containing various amounts of Zn^{2+}. In most cases, the current density was held constant at 250 A m^{-2} for 180 min. This corresponds to a theoretical deposit thickness of 8.5 μm. As can be seen in Figure 1, the morphology of copper deposits differs slightly, but significantly, in the presence of Zn^{2+} (Figure 1(b) and (c)) as compared with that obtained in their absence (Figure 1(a)).

In all cases, the deposits consisted of rounded hillocks. Each hillock most probably corresponds to a single copper crystal. It can be observed that the presence of Zn^{2+} ions in the plating bath induces an increase in

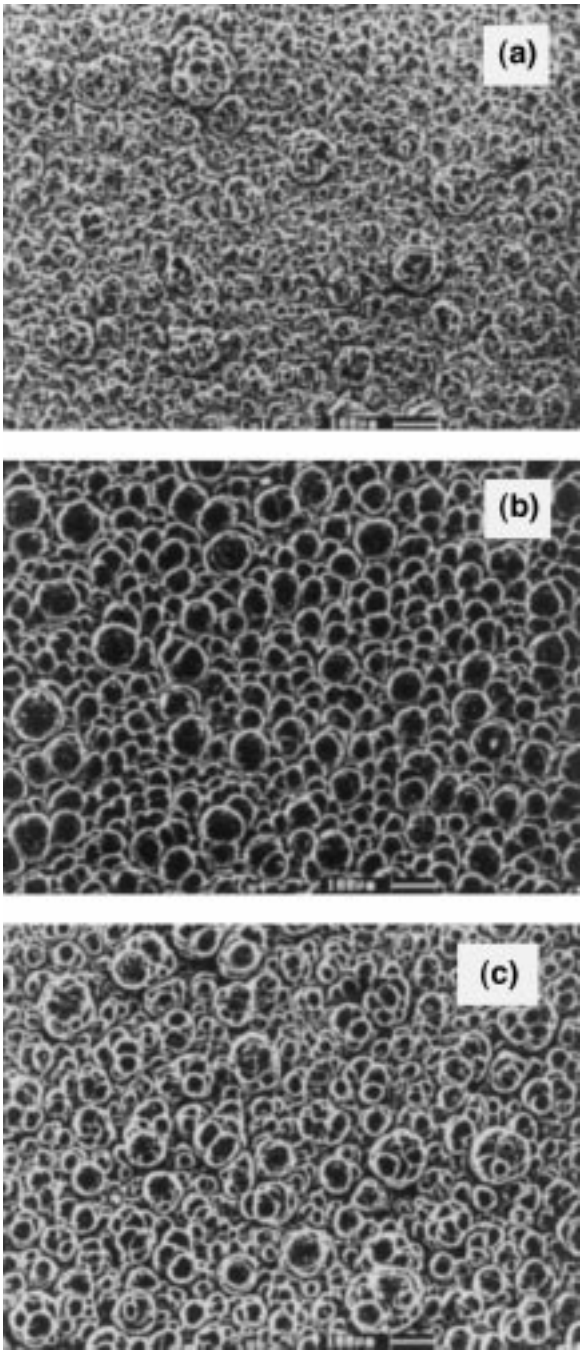

Fig. 1. SEM micrographs of copper electrodeposits obtained from sulphate electrolyte without (a) and with different concentrations of Zn^{2+} ions: (b) 50 mg dm^{-3}; (c) 500 mg dm^{-3}.

grain size D_g ($D_g = 25\ \mu m$ for $c_{Zn} = 0$ to $D_g = 75\ \mu m$ for $c_{Zn} = 500\ \mu g\ dm^{-3}$) which is modified in the presence of Zn^{2+}. Zinc was never detected in the copper deposits by EDX analysis, even for the largest concentrations in the bath. According to X ray diffraction, in contrast to electrodeposits of other metals, these copper electrodeposits did not exhibit a clear preferential orientation. In all cases, the X ray diagrams were very similar to that of a randomly oriented powder and the presence of Zn^{2+} in the bath did not change the relative heights of the diffraction peaks. These initial results show that the foreign ions are present at the interface. They disturb the growth mechanism of copper although they are not codeposited. However, the electrosorption of Zn^{2+} is probably independent on the orientation of crystal faces and therefore, has no influence on the growth direction. The observed effects occurred for small Zn^{2+} additions and were not significantly increased for larger concentrations up to 500 mg dm^{-3}.

3.2. *Cyclic and linear voltammograms*

Cyclic voltammograms for copper deposition/dissolution, from solutions without and with 30 mg dm^{-3} Zn^{2+}, were recorded using a motionless copper disc electrode (Figure 2). When the potential became more negative, an increase in the cathodic current density due to copper electrodeposition was initially observed, and was followed by a decrease due to the establishment of the Nernst diffusion layer. A symmetrical behavior was observed on the anodic part of the curve. After addition of Zn^{2+}, an increase in the cathodic and anodic peak surface of about 10% was observed. This phenomenon can be attributed either to an increase in the surface roughness of the copper deposits or to activation of the surface reactions.

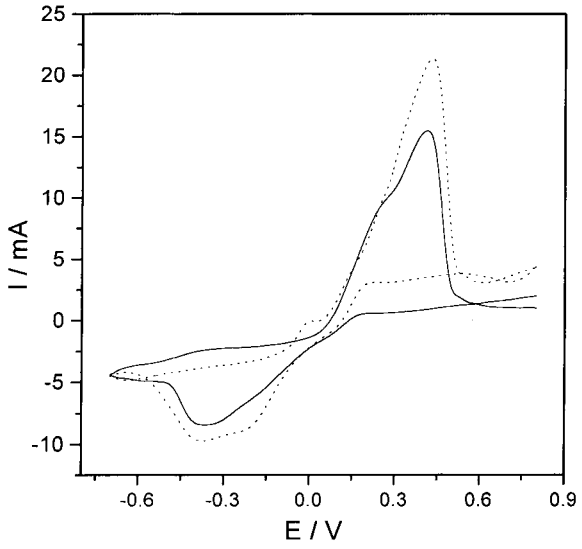

Fig. 2. Cyclic voltammograms for 20 mV s^{-1} scan rate on various Zn^{2+} concentrations: continuous line – 0 mg dm^{-3}, dotted line – 30 mg dm^{-3}.

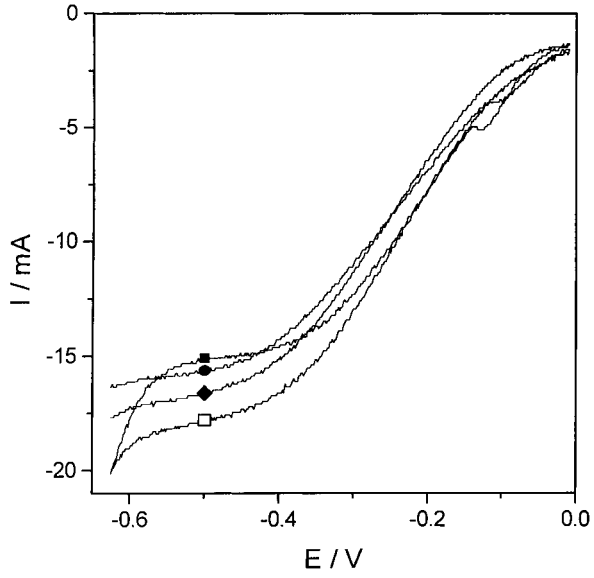

Fig. 3. Polarization curves using various Zn^{2+} concentrations: (■) 0 mg dm^{-3}, (●) 30 mg dm^{-3}, (◆) 100 mg dm^{-3}, (□) 500 mg dm^{-3}. Rotation speed 1300 rpm, scan rate 20 mV s^{-1}.

Cathodic linear polarization curves were recorded without ohmic drop compensation, by rotating the disc electrode up to 1300 rpm in order to verify effects of mass transport. The significant increase of the limiting current intensity for $E < -0.5$ V vs SCE caused by the presence of Zn^{2+} ions is clearly an effect of higher roughness leading to an increase in the effective surface area. The small differences between the various curves in the part which is not under mass transport control, are probably due to small differences in electrolyte resistance, due to changes in electrode positioning. They cannot be attributed to a change in the exchange reaction rate.

3.3. *Impedance measurements*

Electrochemical impedance analysis was used to characterize in more detail the effects of electrosorbed zinc ions on the elementary steps of the copper electrodeposition process. Experimental impedance diagrams presented in the complex-plane (Figures 4–6), recorded in the above mentioned polarization and addition concentration range, exhibited two capacitive loops and an additional low-frequency inductive loop. No important modification of the shape, type and number of the loops

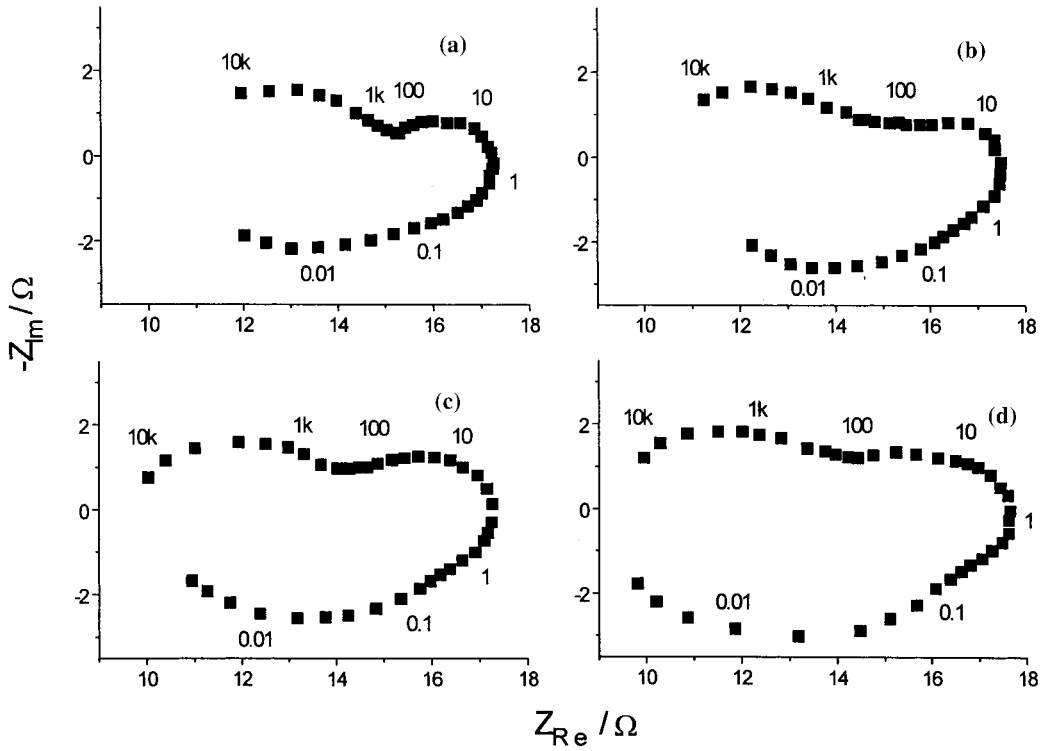

Fig. 4. Complex-plane impedance diagrams for copper electrodeposition at $E = -0.1$ V. Rotation speed 1000 rpm, Zn^{2+} ions concentration: (a) 0 mg dm^{-3}, (b) 10 mg dm^{-3}, (c) 30 mg dm^{-3}, (d) 100 mg dm^{-3}. Frequencies in Hz ($i = 88$ mA cm^{-2}).

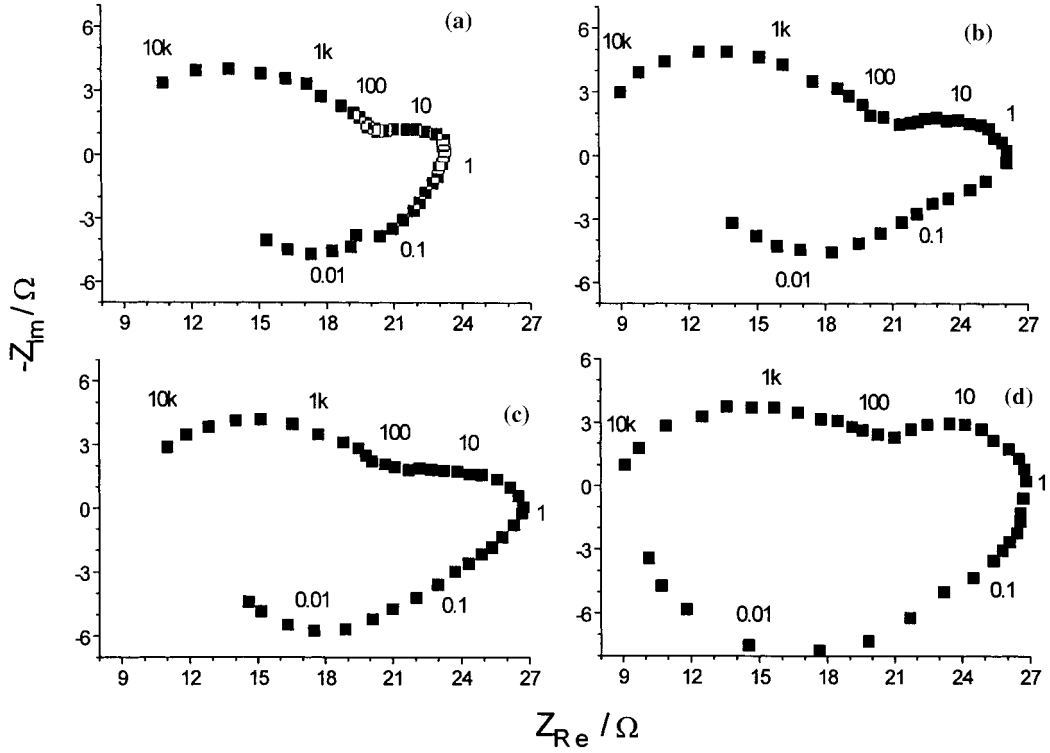

Fig. 5. Complex-plane impedance diagrams for copper electrodeposition at $E = -0.075$ V. Rotation speed 1000 rpm, Zn^{2+} ions concentration: (a) 0 mg dm^{-3}, (b) 10 mg dm^{-3}, (c) 30 mg dm^{-3}, (d) 100 mg dm^{-3}. Frequencies in Hz ($i = 78$ mA cm^{-2}).

was observed, but only slight modifications of the apex loop and diameter are evident for different Zn^{2+} concentrations at all potentials.

The high-frequency loop, due to the finite rate of the charge transfer across the interface, allows the determination of the charge transfer resistance, R_{ct} and the capacitance of the double layer, C_d. The values of these parameters were determined by a Levenberg–Marquardt procedure of nonlinear fitting using a model consisting of a parallel network between a resistor and a capacitor connected in series with an additional resistor. The fitted experimental data were limited to a total of 5–6 points, with the frequency values centered on the apex.

To demonstrate the electrosorption of the Zn^{2+} ions, the adsorption capacitance, C_a, was calculated. In contrast to the case where the adsorbed species is involved in the electrode reaction [12], for the electrosorption of an indifferent species, the double layer capacitance is independent of frequency. Because the electrosorption of a charged species increases the charge separation at the interface, the adsorption capacitance can be obtained by subtraction of the estimated double layer capacitance in the absence of the Zn^{2+} ions, C_d^*, from the value obtained in its presence:

$$C_a = C_d - C_d^* \tag{1}$$

The above relation does not take into account any change in the electrode surface. If the mentioned effect is important, a better possibility is to use a similar equation that contains the extensive parameters obtained after normalization of the capacitances to the continuous component of the current intensity. Because an increase in the active area will affect both the double layer capacitance and the current intensity, the extensive parameter C/I will not be so affected by the changing surface, assuming that the charge transfer kinetics are unchanged.

A slight reduction in charge transfer resistance (Figure 7(a)) and an increase in the adsorption capacitance of Zn^{2+} ions, even at low concentration values (Figure 8(a)) were observed. Using the empirical model: $C_a = Ac_{Zn^{2+}}^N$, Table 1 presents the values of A and N, obtained by fitting experimental data to the model. The corresponding standard errors, correlation coefficient, R, and the value of the double layer capacitance in the absence of Zn^{2+} ions are also presented.

Figures 7(b) and 8(b) show the variation of the parameters IR_{ct} and C_d/I with Zn^{2+} concentration. Because the variation of the current density induced by

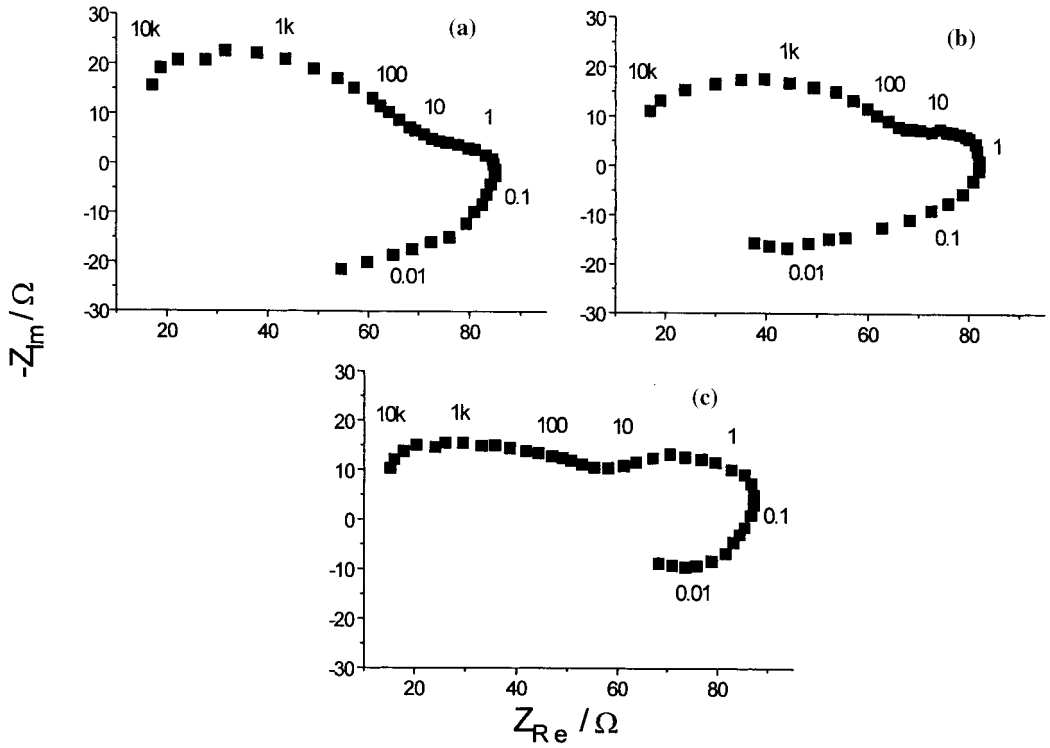

Fig. 6. Complex-plane impedance diagrams for copper electrodeposition at $E = -0.05$ V. Rotation speed 1000 rpm, Zn^{2+} ions concentration: (a) 0 mg dm^{-3}, (b) 10 mg dm^{-3}, (c) 30 mg dm^{-3}. Frequencies in Hz ($i = 67$ mA cm^{-2}).

the presence of the Zn^{2+} ions is small, the modifications of these parameters induced by the surface modification are insignificant by comparison with the modifications of R_{ct} and C_d. Figure 8(b) shows that the reduced parameter C_d/I increases significantly with Zn^{2+} concentration. It can be concluded that this effect results mostly from an increase in the interfacial capacitance due to the presence of adsorbed Zn^{2+} ions, and not from a simple variation in the surface area.

As can be seen from Figures 4–6, the ohmic resistance was not invariant. This is due to the difficulty of maintaining the distance between the working and the reference electrode constant. The resulting ohmic resistance variation was less than 1–2 Ω and caused differences, not exceeding 3–4 mV, between the potentials corrected from the ohmic drop for the different Zn^{2+} concentrations. Similarly, the presence of the additive had a very small influence on the charge transfer resistance and it is difficult to draw a clear conclusion about its influence.

The low-frequency features were interpreted on the basis of a model developed originally for silver electrodeposition [13] and subsequently verified for copper [14]. The presence of two loops, capacitive and inductive, is explained in terms of relaxation of the electrode area due to the birth and growth of monolayers formed on the facets of crystallites. The capacitive loop originates from the propagation of edges over a finite distance, while the inductive loop corresponds to the lengthening of this distance, possibly related to the slow desorption of inhibiting adsorbate species.

This model assumed that:

(i) the birth of edges is a random process characterized by a mean birth rate, v,

(ii) the velocity of edges, v, is proportional to the current density, i, on the active area of edges,

(iii) the active edges grow radial and the length of active edge is governed by an ageing function $f(u, \tau)$, where u is the age of a monolayer and τ its lifetime, corresponding to the mean propagation distance of edges, r_o, given by

$$r_o = v\tau \tag{2}$$

(iv) the propagation distance r_o lengthens with increasing overpotential and τ_n is the time delay necessary for this lengthening.

Assuming that the steady state is reached, the faradaic impedance, Z_f, is given by

$$\frac{1}{Z_f I} = \frac{1}{R_{ct} I} + \left(\frac{dv}{v dE} - \frac{dv}{v dE}\right)\frac{F(\omega)}{\tau} \tag{3}$$

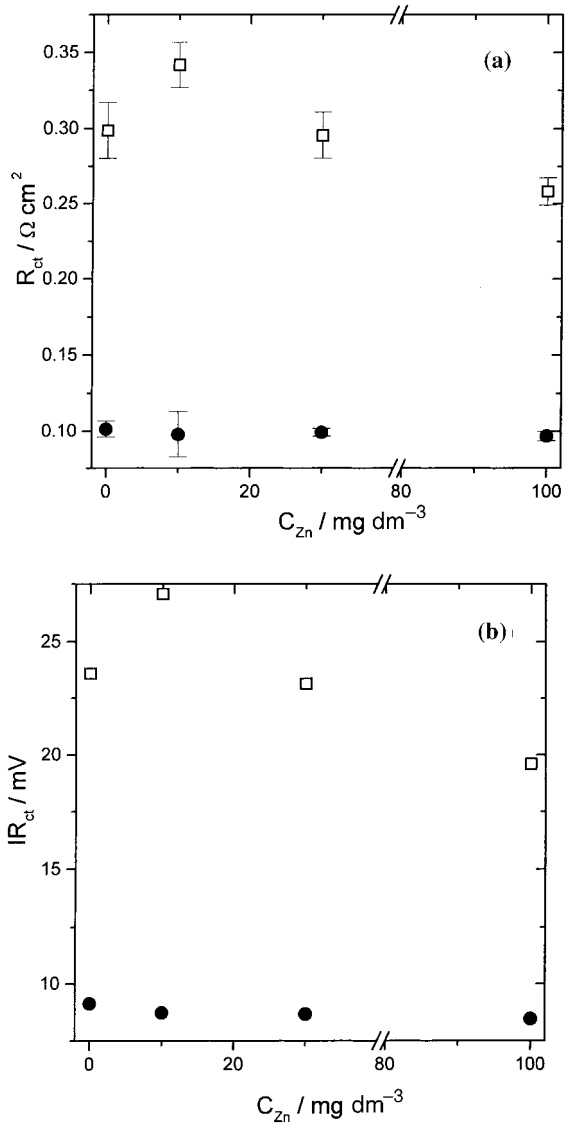

Fig. 7. Influence of Zn^{2+} ion concentration on the charge transfer resistance (a), and on intensive parameter IR_{ct}, (b). D.c. potential: (□) −0.075 V, (●) −0.1 V. Error bars indicate the calculated standard error.

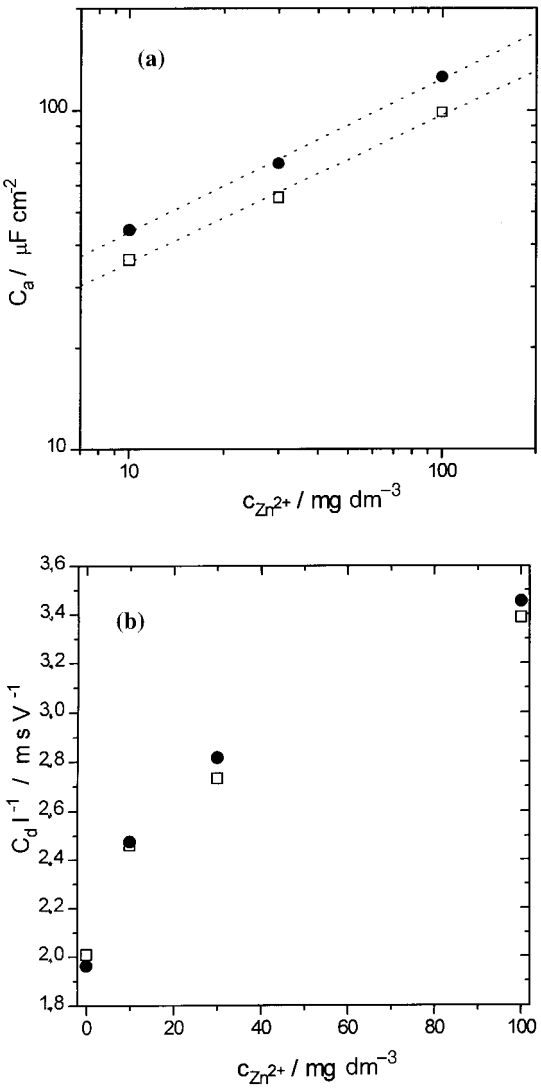

Fig. 8. Influence of Zn^{2+} ion concentration on the adsorption capacitance (a), and on intensive parameter C_d/I (b). D.c. potential: (□) −0.075 V, (●) −0.1 V.

where I is the current intensity, E is the applied potential and R_{ct} is the charge transfer resistance. The Fourier transform of the ageing function is given by

$$F(\omega) = \int_0^\infty f(u,\tau)\exp(-j\omega u)\,du \tag{4}$$

The inductive or capacitive type of process response depends on the differences between the differentials contained in the faradaic impedance equation. Therefore, if the inequality:

$$\frac{dv}{v dE} > \frac{dv}{v dE} \tag{5}$$

is satisfied, an inductive loop will be generated and, in the reverse case, a capacitive one.

Considering the fraction of nuclei, λ, subject to delay τ_n before entering into an ageing process, the faradaic impedance equation becomes a function of the two time constants, τ and τ_n: [15]

$$\frac{1}{Z_f} = \frac{1}{R_{ct}} + \left[\frac{1}{R_p}\left(\frac{\lambda}{1+j\omega\tau_n} + 1 - \lambda\right) - \frac{1}{R_{ct}}\right]\frac{F(\omega)}{\tau} \tag{6}$$

where R_p is the polarization resistance, obtained by extrapolation of Z_f at infinite low frequencies. The delay

Table 1. Double layer capacitance values and standard errors determined in the absence of Zn^{2+} ions and the coefficients values, standard errors with correlation coefficient, R, describing the influence of Zn^{2+} ions on the adsorption capacitance

E/V	A		N		R	$C_d^*/\mu F\ cm^2$	
	Value	Std. error	Value	Std. error		Value	Std. error
−0.075	13.0	1.2	0.435	0.027	0.9981	158	29
−0.100	15.0	1.3	0.455	0.022	0.9980	177	31

τ_n includes any retarding process such as the induction time of nucleation, the slow desorption of inhibiting species or any other retarding event.

If the epitaxial growth is perturbed by the electrode surface roughness or by poor electrode polishing, the low-frequency loop becomes inductive as disordered polycrystalline deposits are formed. Therefore, the LF inductive loop, characterized by the nucleation time-constant, τ_n, is strongly influenced by the growth mode of the deposit.

From this analysis it appears that the time constant τ_n is influenced by the additive concentration (Figure 9). A significant decrease was found, especially at low concentration, suggesting that the adsorbed Zn^{2+} ions modify the birth of edges. This behavior was previously attributed to a slow desorption of some inhibiting species, a process equivalent to an elongation of r_0 with the potential [15]. The decrease in τ_n suggests a stimulation of the desorption of an inhibiting species at the electrode in the presence of Zn.

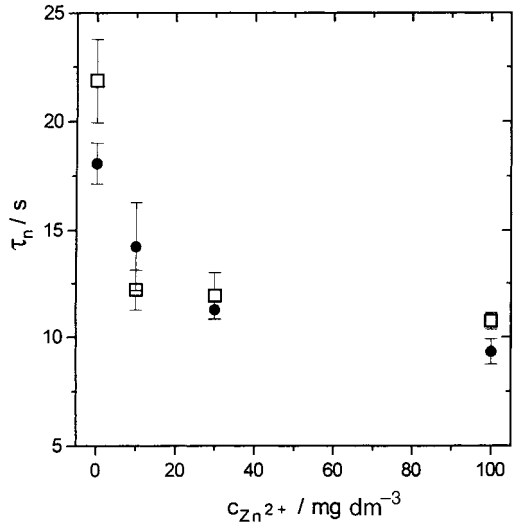

Fig. 9. Influence of Zn^{2+} ion concentration on the nucleation time constant τ_n. D.c. potential: (□) −0.075 V, (●) −0.1 V. Error bars indicate the calculated standard error.

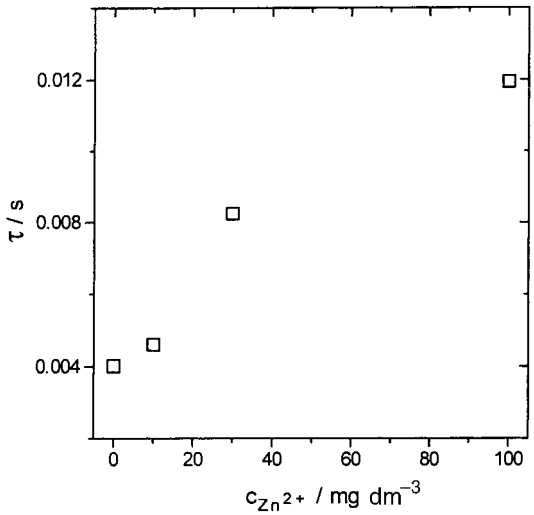

Fig. 10. Influence of Zn^{2+} ion concentration on the time constant of the low-frequency capacitive loop, τ, for $E = -0.075$ V.

Due to the small extent of the frequency domain, λ was not precisely determined. It was found to be in the range 0.95–1, excluding the situation where additive concentration is high at the lowest overpotential value (Figure 6(c)), which corresponds to the cases when the polarization resistance had a much lower value than R_O (the resistance when the capacitive behaviour turns into inductive behaviour).

The time constant of the low frequency capacitive loop, is strongly influenced by the Zn^{2+} concentration (Figure 10). Its characteristic frequency lies in the range of few hertz. As suggested in [14], this low frequency capacitive loop is not a consequence of nucleation growth phenomena, but of the kinetic effects of the two step reduction process of Cu^{2+} ions. The small variations in the loop parameters suggest that the adsorbed Zn^{2+} ions slightly modify the two standard heterogeneous rate constants corresponding to the above mentioned successive reactions.

4. Conclusions

An influence of zinc on copper deposit morphology, was detected, in spite of the fact that, due to the largely different reduction potentials of Zn^{2+} and Cu^{2+} ions, the codeposition of the two metals is theoretically impossible.

The morphology of copper deposits differs slightly in the presence of Zn^{2+}. This suggests that Zn^{2+} ions are electrosorbed at the interface and slightly modify the microscopic aspect and, consequently, the effective surface of the copper deposits. The changes occur at small Zn^{2+} additions and there are no significant

differences between the deposits obtained with 50 and 500 mg dm^{-3} Zn^{2+} concentrations.

An increase in the cathodic peak surface in cyclic voltammograms is observed in the presence of Zn^{2+}, which is in agreement with the higher roughness of the copper deposits obtained in a parallel plate electrolysis cell.

Impedance spectroscopy measurements reveal the presence of a high frequency capacitive loop (allowing the determination of the double layer capacitance and of the charge transfer resistance), of a low frequency capacitive loop, caused by the two-step charge transfer of the copper ions, and of a low frequency inductive loop, that can be used for the quantification of the growth model of the deposit. In order to demonstrate the electrosorption of the Zn^{2+} ions, the adsorption capacitance, C_a, was calculated and correlated with Zn^{2+} concentration. The presence of the Zn^{2+} ions increases the value of the double layer capacitance. Due to the slight variation of the dc intensity with ion concentration, we concluded that in the variation of the double layer capacitance the electrosorption effect is dominant. The charge transfer resistance is slightly affected by the presence of Zn^{2+} ions. The most important effect on the copper electrodeposition kinetics seems to be the modification of the balance between the two steps of the reduction of Cu^{2+} ions. It was found that the nucleation time constant is influenced by the concentration of Zn^{2+}, especially at low concentrations (less than 30 mg dm^{-3}). The presence of Zn^{2+} ions induces a decrease in the nucleation time constant, probably by stimulation of the desorption of an inhibiting species.

Acknowledgements

We thank Dr R. Wiart, from UPR 15 du CNRS (Paris) for helpful discussions concerning the impedance measurements and for his critical remarks and help during the revision of the manuscript.

References

1. T. Subbayah and S.C. Das, *Hydrometallurgy* **36**(3) (1994) 271.
2. R.S. Kaplan, 'Recycle and Secondary Recovery of Metals', edited by P.K. Taylor, H.Y. Sohn and N. Jarett (TMS–AIME, 1985), p. 3.
3. Gh. Facsko, Electrochemical Technology, Ed. Tehnica Bucuresti (1969).
4. R.O. Loutfy and N.M. Bhamcha, *Can. Patent 1 077 884 (Cl. C25C1/12)* (1980).
5. R.O. Loutfy and N.M. Bhamcha, *US. Patent 4 124 460 (Cl. C25C1/12)* (1978).
6. M.S. Quraishi and T.S. Fahidy, *Chem. Ind.* **9** (1975) 377.
7. H.E. Eguez and E.H. Cho, *J. Met.* **39**(7) (1987) 38.
8. R. Kehl, W. Schwab, R.B. Sudderth and G.A. Kordosky, *Ger. Offen. DE 3 836 731 (ClC25C1/20)* (1990).
9. D.Z. Suleimanova and G.V. Makarov, *Tr. Khim. Metall. Inst. Akad. Nauk. Kaz. SSR,* **24** (1974) 13.
10. Bimaghra and J. Crousier, *Mater. Chem. Phys.* **21** (1989) 109.
11. L. Muresan, L. Oniciu, M. Froment and G. Maurin, *Electrochim. Acta* **37**(12) (1992) 2249.
12. M. Sluyters-Rehbach, *Pure & Appl. Chem.* **66** (1994) 1831.
13. C. Cachet, C. Gabrielli, F. Huet, M. Keddam and R. Wiart, *Electrochim. Acta* **28** (1983) 899.
14. E. Chassaing and R. Wiart, *Electrochim. Acta* **29** (1984) 649.
15. R. Wiart, *Electrochim. Acta* **35** (1990) 1587.